CHAPTER IV

STRUCTURAL ASPECTS OF SBA-1 CUBIC MESOPOROUS SILICA SYNTHESIZED VIA A SOL-GEL PROCESS USING SILATRANE PRECURSOR

4.1 Abstract

Silatrane prepared from fumed silica and triethanolamine (TEA) was used as a precursor for SBA-1 synthesis at room temperature using cationic surfactants, derived from alkyltrimethylammonium bromides, C_nTMAB (n = 14, 16 and 18), as templates in dilute solutions. The influences of acidity, alkyl chain length of the surfactant and synthesis temperature were studied. The shape of the SBA-1 crystals was dependent on alkyl chain length of the surfactant. At high surfactant concentration and elevated reaction temperature (50°C), three-dimensionally ordered mesopores were invariably produced. Both X-ray diffraction and transmission electron microscopic results showed the characteristics of the three-dimensional cubic structure. Scanning electron microscopic images of SBA-1 indicated the crystalline-like appearance of an octadecahedron (18-hedron) consistent with 6 squares {100} and 12 hexagons {110} planes consistent with a cubic symmetry. The surface area of the product was as high as 1000–1500 m^2/g with an adsorption volume of 0.6 – 1.0 cm^3/g.

4.2 Introduction

Since the discovery of M41S silicas, many researches have been concentrated on this new class of mesoporous materials [1,2]. It is well known that SBA-1 is analogous to a cubic assemblage of globular micelles in amphophilic surfactant solutions and has a structure suggested being a cage type with open windows [3-5]. Generally, SBA-1 mesoporous silicas were synthesized using tetraethoxysilane (TEOS) as the silica source and a hexadecyltriethylammonium

bromide (C_{16}TEABr) template with a large head group in highly acidic conditions [6,7].

However, many researchers have concentrated SBA-1, as compared to other mesoporous materials such as MCM-41, FSM-16 and SBA-3 [8], possibly because many large head group of surfactants are not commercially available. Kim and Ryoo [3] reported that cubic SBA-1, with good three-dimensional order, could be synthesized using alkyltrimethylammonium chloride (C_nTMACl) as a surfactant, and found that low temperatures were favorable for the formation of a high-quality product. Che et al. [9] examined the effect of counter ions on mesophase formation and succeeded in the synthesis of highly ordered SBA-1 materials with 54 or 74 facets that assumed cubic $Pm\bar{3}n$ symmetry formed through ordering of mesopore layers with *p6mm* planar symmetry [10]. Subsequently, they found that mesostructure formation was strongly dependent on acid concentration and presented a procedure for synthesizing SBA-1 using hexadecyltrimethylammonium bromide (C_{16}TMAB) as the template [4]. Chao et al. [11] introduced a new concept to synthesize high-quality SBA-1 mesoporous silica in a dilute solution from commercially available alkyltrimethylammonium surfactant and sodium silicate.

In this study, we introduce silatrane as a silica source for the synthesis of SBA-1. While, silatrane has been used successfully as a precursor for synthesis of microporous [12-15] and mesoporous zeolites [16,17] via sol-gel processes, This paper describes the preparation of remarkably high quality of SBA-1 and the influence of acidity, alkyl chain length of the templates and temperature on formation and morphology.

4.3 Experimental

4.3.1 Materials

The silatrane precursor was synthesized from fumed silica (99.8%, Sigma-Aldrich) and triethanolamine (TEA) (Carlo Erba) reactants; ethylene glycol (EG) (J.T.Baker) was used as the solvent, and acetronitrile (Labscan, Asia) as an agent for silatrane purification. Mesoporous SBA-1 was synthesized from the silatrane and

alkyltrimethylammonium bromide (C_nTMAB) (Sigma-Aldrich) used as the template, with H_2SO_4 and NaOH (Labscan, Asia) employed as catalysts.

4.3.2 Synthesis of silatrane precursor

Following the method of Wongkasemjit's group [18,19], silatrane was synthesized directly by mixing SiO_2 and TEA in a simple distillation set using ethylene glycol solvent via the Oxide One Pot Synthesis (OOPS) process. The reaction took place at the boiling point of ethylene glycol (200°C) under a nitrogen atmosphere to remove water as a by-product along with ethylene glycol from the system. The reaction was run for 10 h, after which the remaining ethylene glycol was removed under vacuum at 110°C to obtain a brown solid. The crude product was washed with acetonitrile and dried in a vacuum desiccator before characterization with a Bruker Optics EQUINOX55 fourier-transformed infrared (FT-IR) absorption spectrometer at a resolution of 2 cm^{-1}, and a DuPont 2950 thermogravimetric analyzer (TGA) using a heating rate of 10°C min^{-1} from room temperature to 750°C in a nitrogen atmosphere.

The FT-IR bands observed were 3000-3700 cm^{-1} (w, νO-H), 2860-2986 cm^{-1} (s, νC-H), 1244-1275 cm^{-1} (m, νC-N), 1170-1117 (bs, νSi-O), 1093 (s, νSi-O-C), 1073 (s, νC-O), 1049 (s, νSi-O), 1021 (s, νC-O), 785 and 729 (s, νSi-O-C) and 579 cm^{-1} (w, νN→ Si). TGA showed one sharp mass loss transition at 390°C and gave 18.5 % ceramic yield corresponding to $Si((OCH_2CH_2)_3N)_2H_2$. (Scheme 4.1)

4.3.3 Synthesis of mesoporous SBA-1

The synthesis procedure was as follows. Solution A was prepared by adding the required amount of C_nTMAB (n = 14, 16 and 18) to water (30 ml) and stirring for 0.5 h to obtain a clear solution. Solution B was prepared by adding silatrane (1.4g, 5 mmol) to 14 ml of H_2SO_4 (0.3 – 0.5 M) and NaOH (0.068g, 1.7 mmol), and stirring for 0.5 h to obtain a homogeneous solution. pH values of the solution B is in the range of 1.5 – 2 around the isoelectric point (IEP) of silica. The solution B was then

added to the solution A under vigorous stirring that was continued for 4 h. Before leaving the mixture at room temperature, water (30 ml) was added into the solution mixture. Then the mixture was allowed to age for 1-2 days at the desired temperature to form white precipitates. The products were filtered and washed with distilled water and dried overnight in air. Template removal was achieved by calcination at 560°C for 6 h using a Carbolite Furnace (CFS 1200) with a heating rate of 0.5°C/min. The mixture composition in molar ratio was $1.0C_nTMAB{:}5SiO_2{:}1.7NaOH{:}xH_2SO_4{:}3680H_2O$.

The mesoporous products were characterized using a Rigaku X-ray diffractometer (XRD) at a scanning speed of 1 degree/sec using CuKα radiation on the range of 2θ = 1.5-8°. SBA-1 morphology was observed by secondary electron imaging with a JEO 5200-2AE scanning electron microscope (SEM), while mesopore order was directly examined using a JEOL 2010F Transmission electron microscope (TEM). Surface area and average pore size were determined by the Brunaues-Emmett-Teller (BET) method with a Quantasorb JR instrument.

4.4 Results and Discussion

SBA-1 mesoporous silica was synthesized using the C_nTMAB with n = 14, 16 and 18 as a template under dilute solution of acid, to examine the influence of alkyl chain length on product quality. In addition, acidity and temperature were varied systematically to optimize yield and perfection.

4.4.1 Effect of the acidity

Since SBA-1 morphology depends on the concentration of acid [20], the gel composition ($C_{16}TMAB$: 5Si: 1.7NaOH: xH_2SO_4: $3680H_2O$) was varied over the range at x = 0.3 – 0.5 M. Huo et al [6] proposed the formation of the silica-surfactant mesophase under acidic conditions via an $S^+X^-I^+$ pathway at pH < 2 or through an $S^+X^-I^\circ$ pathway at pH = 2 (S, X and I correspond to surfactant, halide and inorganic species, respectively), leading to variety of topological constructions [21]. In the

present case, with acid concentration varied from 0.3 to 0.5 M, all samples were well ordered with three distinct XRD peaks at 1.5 - 3°, which could be {200}, {210} and {211} reflections of a cubic unit cell with a = 83 Å based on the SBA-1 of $Pm\bar{3}n$ mesostructure [22]. Other peaks in the higher angle range of 3 - 6° indicate a high degree of the cubic mesostructured organization. The diffracted intensities declined with increasing the concentration of acid. The SBA-1 particles synthesized at 0.5 M H_2SO_4 were spheres, and those at decreased acid concentration (0.3 M) took on an octadecahedral form (Fig.4.1). These results are in agreement with the observations of Chao et al. [23], who suggested that the growth of SBA-1 facets can be regarded as self-assembly process where the surfactant aggregates and silicate species take on specific orientations at particular pH. In dilute acid solutions, the oligosilicate species are isolated and do not condense appreciably, allowing the surfactant aggregates and silicate species to self-assemble in solution and leading to catalyzed silica condensation. In this condition, being close to the isoelectric point of silica, slow condensation takes place the differentiation of mesopore surfaces and the formation of cuhedral particles (Fig.4.1a). At higher pH, the condensation rate accelerates leading to rapid isotropic growth and anhedral surfaces.

The external shape of the SBA-1 crystals reflected the perfect mesopore order. TEM images of the products that use 0.3 and 0.5 M typically showed that domains of regular mesopores were extensive in the latter material (Fig.4.2)

4.4.2 Effect of alkyl chain length in the surfactant molecules

For all combinations of C_nTMAB surfactant concentration (0.02–0.06 M) and alkyl chain length (n = 14, 16 and 18) in 0.3 M H_2SO_4, well-ordered SBA-1 mesoporous silica was obtained. The surfactant having the longest alkyl chain displayed the narrowest diffraction peaks and higher intensity indicative of superior long-range mesopore order. However, the diffracted intensities were not significantly altered as a function of surfactant concentration in agreement with Chao et al. [11]. These workers found a transformation from a three-dimensionally ordered $Pm\bar{3}n$ phase to a planar structure that retained hexagonal *p6mm* symmetry at a surfactant concentration of 0.06 M, when using the $C_{16}TMAB$ and $C_{18}TMAB$ as templates.

However, the silatrane precursor generates TEA molecule in the solution allows space symmetry to be preserved even at the high template concentration. In addition, structural order for the cubic mesophase was enhanced by increasing the alkyl chain length, because self-assembly is controlled by surfactant hydrophobicity (i.e. chain length) and the concentration [24]. This result can be explained in term of the concept of surfactant packing parameter, g [6,7]. The surfactant packing parameter g is given by $g = V/(a_0 l)$, where V is the total volume occupied by the alkyl tail group plus any co-solvent organic molecule between the chains, a_0 is the effective head group area at the micelle surface, and l is the kinetic length of the alkyl chain.

On increasing the chain length, the kinetic length linearly increases along with the volume. However, with TEA molecules penetrating the hydrophilic region, the effective head group (a_0) is expanded. This phenomenon results in a decrease in the g value, favoring the $Pm\bar{3}n$ cubic mesophase. Secondary electron images of SBA-1 templated with C_{14}TMAB, C_{16}TMAB and C_{18}TMAB surfactants clearly show that the former with lower hydrophobicity interacts most strongly with the silica species, leading to rapid condensation, smaller particle size, and poorly developed facets (Fig.4.3a), which is in general [25]. For C_{16}TMAB, since the surface energy difference between the {100} and {110} faces is not large, the condensation is slower and octadecahedron crystals are formed [26]. An effect is more pronounced for the C_{18}TMAB material. In this latter case, an external decaoctahedron (18-hedron) with 6 square and 12 hexagonal facets is clearly observed [27,28], possibly as C_{18}TMAB gives more counterion association than both C_{16}TMAB and C_{14}TMAB, leading to adequate hydrophilic-lipophilic balance (HLB) [21]; higher hydrophobicity leads to higher counterion condensation and gives better structural ordering in cubic phase. That means, the longer chain length of the surfactant leads to the higher counterion association, which can promote the formation of the greater mesoporous crystal.

The type IV N_2 adsorption-desorption isotherms (Fig.4.4) of the calcined SBA-1 templated by C_{14}TMAB to C_{18}TMAB were similar (Table 4.1) and showed a large increase at relative pressure $P/P_0 = 0.2–0.4$ due to the capillary condensation within uniform mesopores [29, 30]. The pore size and pore volume of SBA-1

increase with the surfactant chain length. For all products, the surface area is high (1000–1500 m^2/g) with an adsorption volume of 0.6–0.95 cm^3/g.

4.4.3 Effect of temperature

As liquid crystal formation is affected by temperature, this parameter was investigated from room temperature to 50°C and correlated with the structural evolution of SBA-1 during synthesis. At 50°C, C_{16}TMAB- and C_{18}TMAB-templated SBA-1 silicas retained the characteristic mesostructure peaks (Fig.4.5B, C). The former templates can be used to synthesize three-dimensionally ordered structures at higher temperatures. Kao et al. [31] studied the phase control of SBA-1 by addition of short-chain alcohols, and found that the alcohol additives served as phase controllers during the high temperature. Rationally, silatrane is a water soluble alkoxide, the hydrolysis of silatrane to silicate species generates TEA molecules in the solution to act as co-template in mesoporous formation. Because the TEA molecules are branch chain and more hydrophilic, they reside on the outer boundaries of the surfactant micelles, making the surfactant micelles less packed and reducing the electrostatic repulsion between the head group. With increasing the temperature, the tail motion increases the effective surfactant volume, leading to increase in the g value. However, the confinement of TEA molecules in the hydrophilic region of the surfactants results in an expansion of the effective head group area (a_0), which balances the effect of the surfactant volume (V), thus the g value, is favor in the formation of cubic SBA-1 phase [31-33]. In addition, SBA-1 templated by C_{14}TMAB material became less ordered at 50°C (Fig.4.5A), and it could be synthesized at lower temperatures than 50°C, since lower hydrophobic C_{14}TMAB can not interact strongly with the silica species at high temperature.

Crystal morphology behavior is also sensitive to temperature. The synthesis at a higher temperature resulted in the formation of a silica-surfactant mesophase with a hexagonal structure [34-37]. Liu et al. [38] observed that a phase transformation occurred from three-dimensionally cubic $Pm\bar{3}n$ to two-dimensionally hexagonal *p6mm* during drying the precipitate. However, in our case, we did not observe the phase transformation (not shown), even when the temperature

was increased to 50°C. In the case of using C_{14}TMAB, most of crystals were octadecahedron, although there were some mosaic-like crystals. For the C_{16}TMAB and C_{18}TMAB, the crystals still had a decahedron shape. This means that the SBA-1 mesoporous silica prepared using the silatrane as a silica source can prevent the morphology change at high temperature because of the generation of TEA molecules as a stabilizer of SBA-1, as discussed above.

4.5 Conclusions

A silatrane precursor has been successfully used to synthesize well-ordered and stable SBA-1 mesoporous silica via the sol–gel method. Under mild conditions with the small head group of CnTMAB, high-quality SBA-1 was produced. The TEA molecules generated from the silatrane precursor significantly influenced the structure of the surfactant micelle by decreasing the surfactant packing parameter

4.6 Acknowledgements

This research work is financially supported by the Postgraduate Education and Research Program in Petroleum and Petrochemical Technology (ADB) Fund, the Ratchadapisake Sompote Fund, Chulalongkorn University and the Thailand Research Fund (TRF).

4.7 References

1. A. Sayari, *Chem. Mater.* 8 (1996) 1840-1852.
2. A. Vinu, V. Murugesan, M. Hartmann, *Chem. Mater.* 15 (2003) 1385-1393.
3. M.J. Kim, R. Ryoo, *Chem. Mater.* 11 (1999) 487-491.
4. S. Che, Y. Sakamoto, O. Terasaki, T. Tatsumi, *Chem. Lett.* 2 (2002) 214-215.
5. Y. Sakamoto, I. Diaz, O. Terasaki, D. Zhao, J. Perez-Pariente, J. M. Kim, G. D. Stucky, *J. Phys. Chem. B.* 106 (2002) 3118-3123.

6. Q. Huo, D.I. Margolese, D.I. Ciesla, D.G. Demuth, P. Feng, T.E. Gier, P. Sieger, A. Firouzi, B.F. Chemelka, F. Schu¨ th, G.D. Stucky, *Chem. Mater.* 6 (1994) 1176-1191.
7. Q. Huo, D.I. Margolese, U. Ciesla, D.G. Demuth, P. Feng, T.E. Gier, P. Sieger, A. Firouzi, B.F. Chemelka, G.D. Stucky, *Chem. Mater.* 8 (1996) 1147-1160.
8. D. Ji, T. Ren, L. Yan, J. Suo, *Mater. Lett.* 57 (2003) 4474-4477.
9. S. Che, S. Kamiya, O. Terasaki, T. Tatsumi, *J. Am. Chem. Soc.* 123 (2001) 12089-12090.
10. S. Che, S. Lim, M. Kaneda, H. Yoshitake, O. Terasaki, T. Tatsumi, *J. Am. Chem. Soc.* 124 (2002) 13962-13963.
11. M.C. Chao, H.P. Lin, D.S. Wang, C.Y. Tang, *Micropor. Mesopore. Mater.* 83 (2005) 269-276.
12. M. Sathupanya, E. Gulari, S. Wongkasemjit, *J. Euro. Ceram. Soc.* 22 (2002) 1293-1303.
13. M. Sathupanya, E. Gulari, S. Wongkasemjit, *J. Euro. Ceram. Soc.* 23 (2003) 2305-2314.
14. N. Phonthammachai, T. Chairassameewong, E. Gulari, A.M. Jameison, S. Wongkasemjit, *J. Met. Mater. Min.* 12 (2003) 23.
15. P. Phiriyawirut, A.M. Jamieson, S. Wongkasemjit, *Micropor. Mesopore. Mater.* 77 (2005) 203-213.
16. N. Thanabodeekij, W. Tanglumlert, E. Gulari, S. Wongkasemjit, *Appli. Organomet. Chem.* 19 (2005) 1047-1054.
17. N. Thanabodeekij, S. Sadthayanon, E. Gulari, S. Wongkasemjit, *Mater. Chem. Phys.* (2005) In Press.
18. V. Jitchum, C. Sun, S. Wongkasemjit, H. Ishida, *Tetrahedron*, 57 (2001) 3997-4003.
19. W. Charoenpinijkarn, M. Suwankruhasn, B. Kesapabutr, S. Wongkasemjit, A.M. Jamieson, *Eur. Polym. J.*, 37 (2001) 1441-1448.
20. P. Srinivasu, S.H. Lim, Y. Kubota and T. Tatsumi, *Cat. Today.* (2006) Inpress.
21. H.P. Lin, C.P. Kao, C.Y. Mou, S.B. Liu, *J. Phys. Chem. B.* 104 (2000) 7885-7894.

22. M.W. Anderson, C.C. Egger, G.J.T. Tiddy, J.L. Casci and K.A. Brakke, *Angew. Chem. Int.*, 44 (2005) 3243-3248.
23. M.C. Chao, D.S. Wang, H.P. Lin, C.Y. Mou, *J. Mater. Chem.* 13 (2003) 2853-2854.
24. K. Holmberg, B. Jonsson, B. Kronberg and B. Lindan, "Surfactants and Polymers in Aqueous Solution" Wiley, England (2002).
25. M.C. Chao, H.P. Lin, D.S. Wang and C.Y. Mou, *Chem. Lett.* 33 (2004) 374-375.
26. H.P. Lin and C.Y. Mou, *Acc. Chem. Res.* 35 (2002) 927-935.
27. S. Guan, S. Inagaki, T. Ohsuna and O. Terasaki, *J. Am. Chem. Soc.* 122 (2000) 5660-5661.
28. S. Guan, S. Inagaki, T. Ohsuna and O. Terasaki, *Micropor. Mesopore. Mater.* 44-45 (2001) 167-172.
29. H.M. Kao, J.D. Wu, C.C. Cheng and A.S.T. Chiang, *Micro. Mesopore. Mater.* 88 (2006) 319-328.
30. H.M. Kao, C.C. Cheng, *Mater. Lett.* (2006) In Press.
31. H.M. Kao, C.C. Cheng, C.C. Ting and L.Y. Hwang, *J. Mater. Chem.* 15 (2005) 2989-2992.
32. M.S. Morey, A. Davidson and G.D. Stucky, *J. Porous. Mater.* 5 (1998) 195-204.
33. H.M. Kao, Y.W. Liao and C.C Ting, *Micro. Mesopore. Mater.* (2006) In Press.
34. M. Ogura, H. Miyoshi, S.P. Naik and T. Okubo, *J. Am Chem. Soc.* 126 (2004) 10937-10944.
35. S. Che, Y. Sakamoto, H. Yoshitake, O. Terasaki, T. Tatsumi, *Micropor. Mesopore. Mater.*85 (2005) 207-218.
36. J. Zheng, S. Zhai, D. Wu and Y. Sun, *J. Solid. Chem.* 178 (2005) 1630-1636.
37. S. Han, W. Hou, J. Xu, X. Huang and L. Zheng, *Chem. Phys. Chem.* 7 (2006) 394-399.
38. M.C. Liu, H.S. Sheu and S. Cheng, *Chem. Commun.* 23 (2002) 2854-2855.

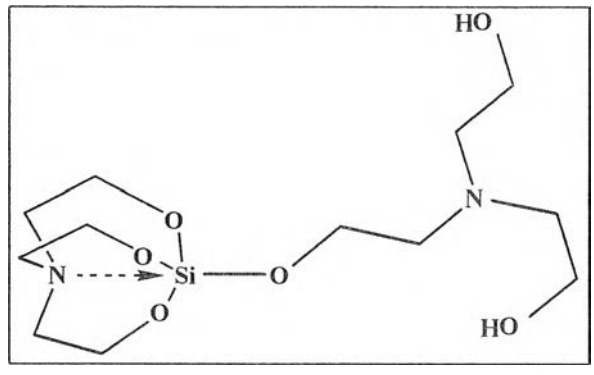

Scheme 4.1 The structure of silatrane.

Table 4.1 BET analysis of SBA-1 synthesized at different surfactant concentrations using 0.3 M H_2SO_4

Surfactant concentration (M)	BET Surface Area (m^2/g)	Pore Volume (cm^3/g)	Average Pore Size (nm)	d_{210} (nm)	a_0 (nm)[a]	D_{me} (nm)[b]
C_{14}TMAB						
0.02	1061	0.50	2.0	3.1	6.9	3.8
0.04	1154	0.60	2.0	3.1	6.9	3.7
0.06	1080	0.65	2.1	3.2	7.2	3.8
C_{16}TMAB						
0.02	1177	0.72	2.1	3.6	8.1	4.6
0.04	1182	0.76	2.1	3.7	8.4	4.7
0.06	1239	0.80	2.1	3.7	8.3	4.7
C_{18}TMAB						
0.02	1297	0.82	2.7	4.3	9.6	5.4
0.04	1435	0.84	2.8	4.4	9.9	5.4
0.06	1520	0.95	2.9	4.4	9.9	5.3

[a] Lattice parameters a_0 were calculated based on the formula $a_0 = \sqrt{5}d_{210}$

[b] Cage diameter was determined by using the equation of $D_{me} = a_0(6\varepsilon_{me}/\pi\nu)^{1/3}$ Dme is the cage diameter of a cubic unit cell of length a_0, ε_{me} is the volume fraction of a regular cavity and ν (ν = 8, for the SBA-1) is the number of cavities present in the unit cell [2,29].

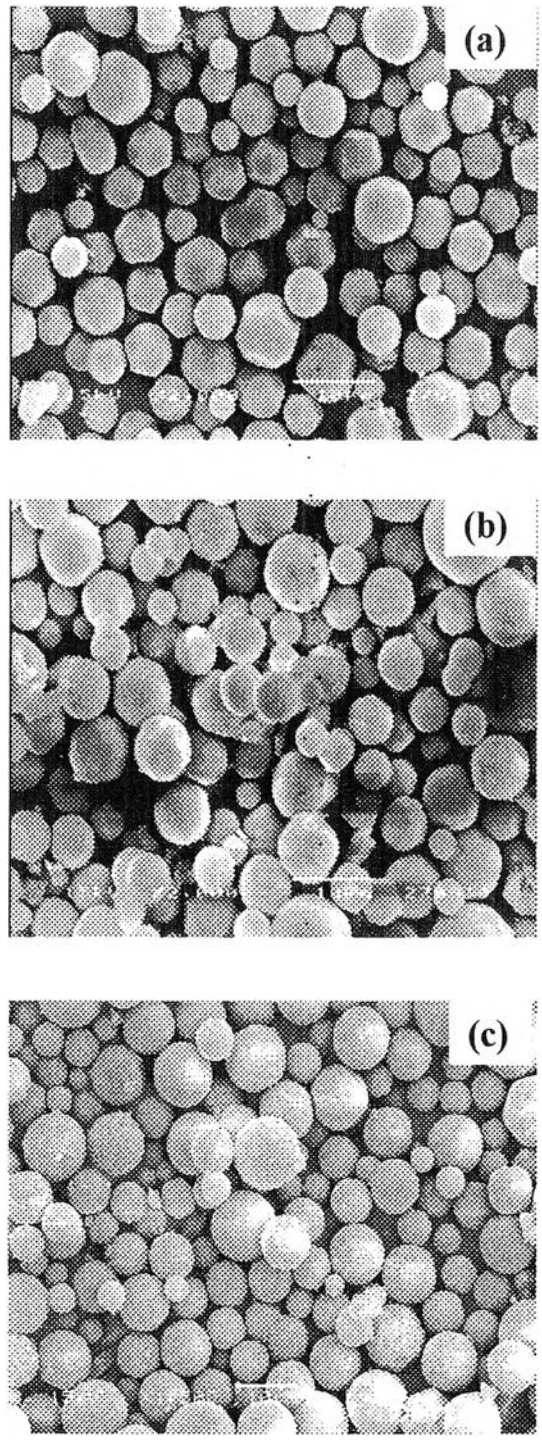

Figure 4.1 SEM micrographs of calcined C_{16}TMAB-templated SBA-1 mesoporous silica using different acid concentrations at room temperature; (a) 0.3, (b) 0.4 and (c) 0.5 M concentration of C_{16}TMAB = 0.04M

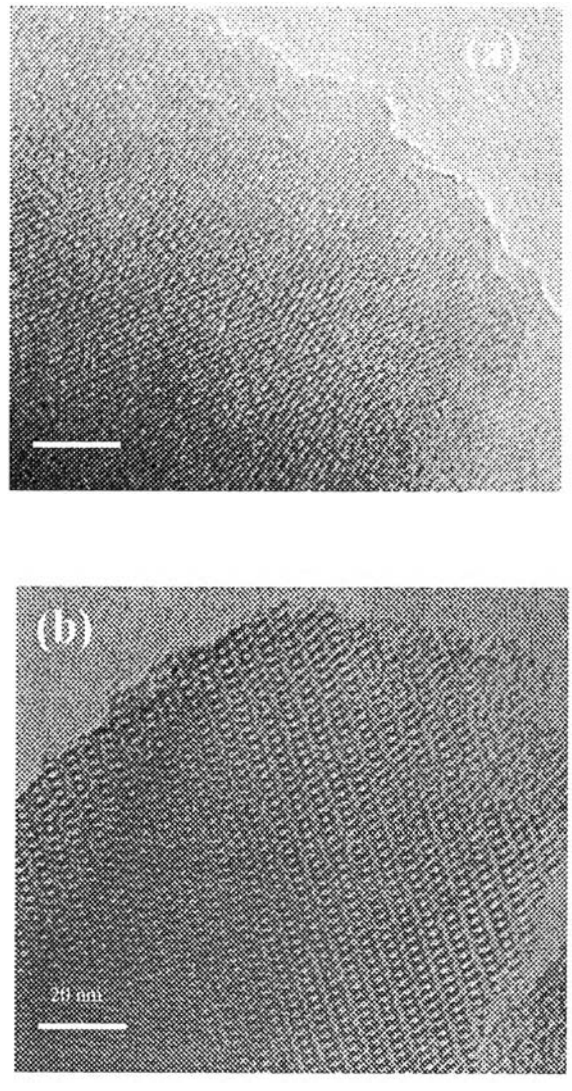

Figure 4.2 TEM images of calcined C_{16}TMAB-templated SBA-1 using different acid concentrations at room temperature;
(a) 0.3 M and (b) 0.5 M concentration of C_{16}TMAB = 0.04M

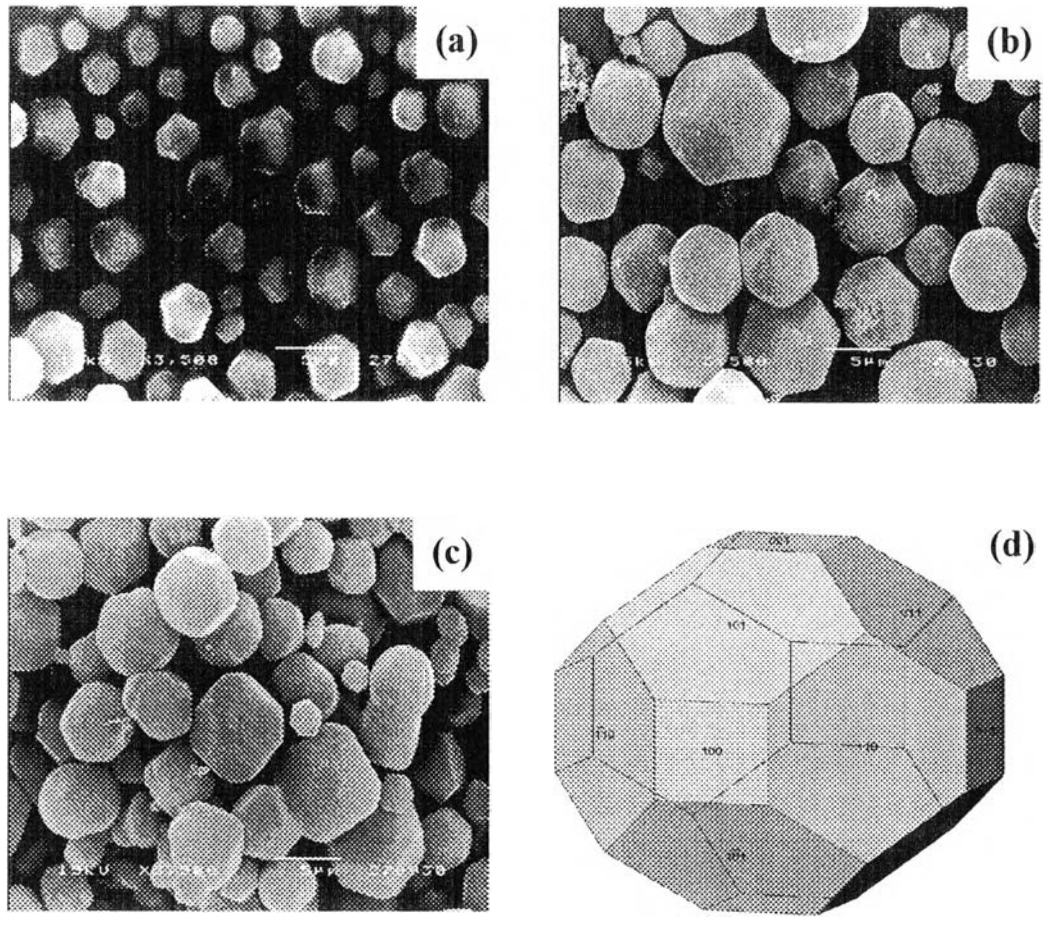

Figure 4.3 SEM micrographs of calcined SBA-1 as a function of the alkyl chain length in the surfactant using surfactant concentration of 0.06 M and 0.3 M H_2SO_4 at room temperature;
(a) C_{14}TMAB, (b) C_{16}TMAB, (c) C_{18}TMAB and (d) a schematic model of SBA-1 particle with the plane indexes

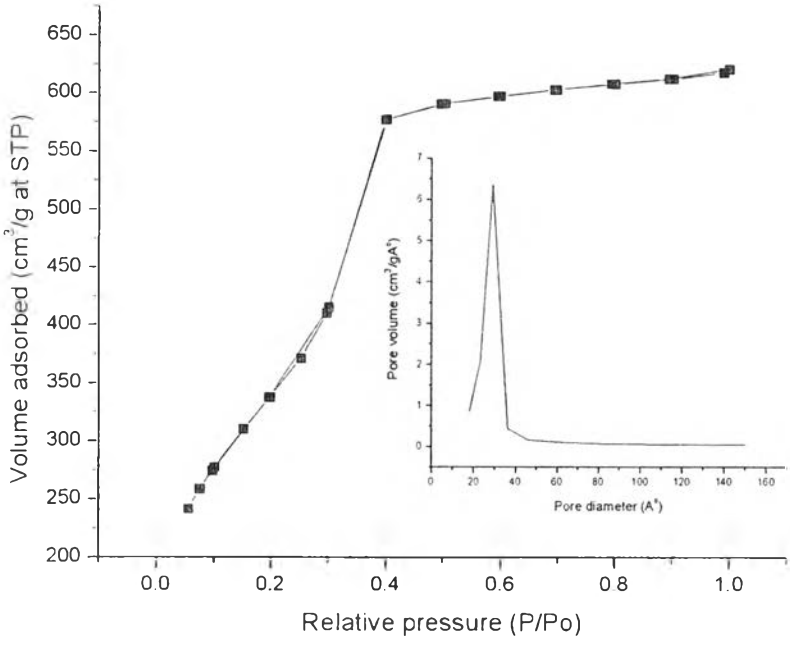

Figure 4.4 A nitrogen adsorption–desorption isotherm and a pore size distribution plot (inset) of calcined C_{18}TMAB-templated SBA-1 synthesized at room temperature using 0.3 M H_2SO_4, 0.06 M C_{18}TMAB

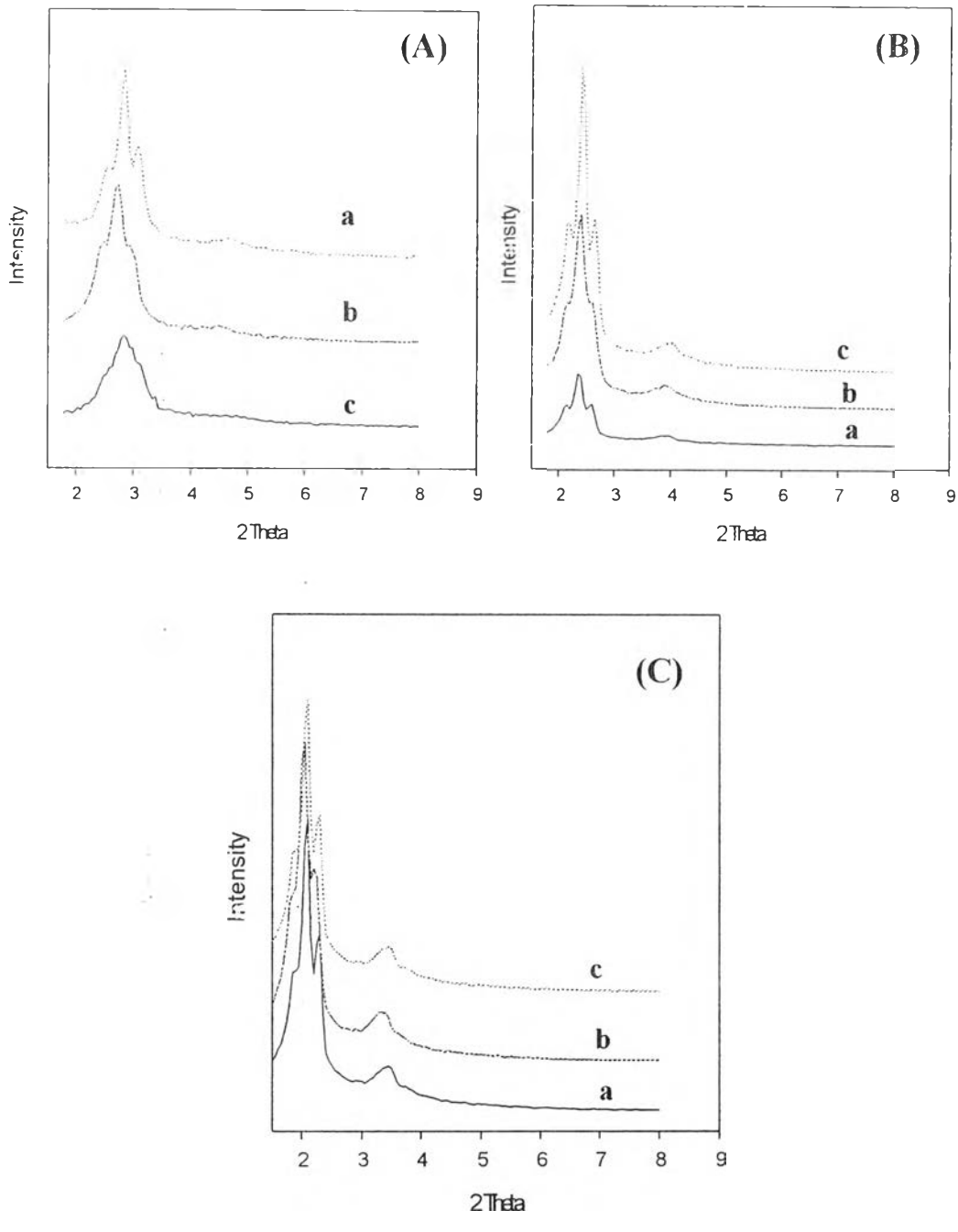

Figure 4.5 XRD spectra of calcined SBA-1 as a function of the reaction temperature and the alkyl chain length in the surfactant at a concentration of 0.06 M using 0.3 M H_2SO_4;
(A) C_{14}TMAB, (a) at room temperature, (b) 40° and (c) 50°C
(B) C_{16}TMAB, (a) at room temperature, (b) 40° and (c) 50°C
(C) C_{18}TMAB, (a) at room temperature, (b) 40° and (c) 50°C